First observation of excited states in the neutron deficient $N=86$ isotones ^{159}Ta and ^{160}W

A. Keenan,[1,*] R. D. Page,[1,†] J. Simpson,[2] N. Amzal,[1] J. F. C. Cocks,[3] D. M. Cullen,[1,‡] P. T. Greenlees,[1,*] S. L. King,[1] K. Helariutta,[3,§] P. Jones,[3] D. T. Joss,[4] R. Julin,[3] S. Juutinen,[3] H. Kankaanpää,[3] P. Kuusiniemi,[3] M. Leino,[3] M. Muikku,[3,‖] A. Savelius,[3] M. B. Smith,[5,¶] and M. J. Taylor[1]

[1]*Oliver Lodge Laboratory, University of Liverpool, Liverpool L63 7ZE, United Kingdom*

[2]*CLRC, Daresbury Laboratory, Warrington WA4 4AD, United Kingdom*

[3] *Department of Physics, University of Jyväskylä, FIN-40351 Jyväskylä, Finland*

[4]*Division of Natural Sciences, Staffordshire University, Stoke-on-Trent ST4 2DE, United Kingdom*

[5]*Department of Physics, University of Paisley, Paisley PA1 2BE, United Kingdom*

(Received 13 February 2001; published 8 May 2001)

The γ decays of excited states in the neutron deficient nuclei ^{159}Ta and ^{160}W have been identified for the first time. The nuclei of interest were produced in reactions induced by beams of ^{58}Ni ions at energies of 286 MeV, 291 MeV, and 298 MeV bombarding a ^{106}Cd target. Prompt γ rays were recorded using the JUROSPHERE spectrometer and were tagged through the subsequent α decays of associated recoil ions measured in a position-sensitive silicon strip detector at the focal plane of the gas-filled separator RITU. Level schemes have been deduced and compared with similar structures observed in neighboring nuclei.

DOI: 10.1103/PhysRevC.63.064309 PACS number(s): 23.20.Lv, 23.60.+e, 27.70.+q

I. INTRODUCTION

The study of excited states of nuclei close to the proton drip line above the $N=82$ shell closure has advanced significantly in recent years [1–3]. Many nuclei in this region decay by α-particle or proton emission [4] and the rapid progress in their study has largely been achieved by tagging the γ rays with the characteristic radioactive decay properties of the associated recoil ions measured at the focal plane of a recoil separator. A major advantage of this method is that often several nuclei produced in a given reaction can be selected cleanly and independently. In the present work, this technique has been applied to study for the first time excited states in the neutron deficient $N=86$ isotones $^{159}_{73}$Ta and $^{160}_{74}$W.

Prior to this investigation, the lightest tungsten isotope in which excited states had been identified by γ-ray spectroscopy was ^{162}W [5]. The systematics of low-lying states in even-mass tungsten isotopes are consistent with a decreasing deformation moving away from the neutron midshell towards the $N=82$ shell closure [6]. This trend is expected to continue for $^{160}_{74}W_{86}$, with the yrast states arising from spin alignments of valence nucleons, as observed in lighter $N=86$ isotones. Data on neutron deficient tantalum isotopes are much scarcer, the lightest isotope studied using in-beam γ-ray spectroscopy being ^{165}Ta [7]. However, the pattern of the lowest-lying excited states in ^{159}Ta is expected to resemble those of its neighboring $N=86$ isotones ^{158}Hf and ^{160}W, with the odd proton coupling to the neutron excitations. The aim of the present work was therefore to determine whether these expectations are indeed followed and to investigate the effects of the increasing number of valence protons on the pattern of excitations.

II. EXPERIMENTAL METHOD

The experiment was performed at the Accelerator Laboratory of the University of Jyväskylä. The nuclei of interest were produced in fusion-evaporation reactions induced by ^{58}Ni ion beams at energies of 286 MeV, 291 MeV, and 298 MeV impinging on a self-supporting 550 μg cm^{-2} thick ^{106}Cd target. The reaction was studied at 291 MeV for approximately 85 h, while data were collected for approximately 16 h at each of the other two beam energies. The beam was pulsed with 1.3 ms beam on and 1.7 ms beam off for the 291 MeV data and 4.8 ms beam on and 5.2 ms beam off for the other two energies. The pulsing allowed clean α-particle energy spectra to be generated so that accurate coincidence requirements could be obtained. In the offline analysis no beam phase conditions were applied to the α decays when producing γ-ray spectra. The average beam intensity after pulsing was typically $\sim$1 particle nA.

Prompt γ rays were detected with the escape-suppressed hyperpure germanium detectors of the JUROSPHERE spectrometer array located at the target position. JUROSPHERE is a composite array of Eurogam phase I germanium detectors [8] at backward angles to the beam direction and TESSA detectors [9] around 90°. In this experiment there were five Eurogam detectors at 157.6° and 9 at 133.6°, with five TESSA detectors at 79° and five at 101°. The efficiencies relative to a standard 76 mm$\times$76 mm NaI(Tl) detector at 25 cm for 1.3 MeV γ rays were 70% and 25% for the Eu-

*Present address: Department of Physics, University of Jyväskylä, P.O. Box 35, FIN-40351 Jyväskylä, Finland.

†Corresponding author. Electronic address: rdp@ns.ph.liv.ac.uk

‡Present address: Department of Physics and Astronomy, University of Manchester, Manchester M13 9PL, United Kingdom.

§Present address: Gesellschaft für Schwerionenforschung, D-6100 Darmstadt, Germany.

‖Present address: CLRC, Daresbury Laboratory, Warrington WA4 4AD, United Kingdom

¶Present address: Department of Physics and Astronomy, Rutgers University, New Brunswick, NJ 08903.

rogam and TESSA germanium detectors, respectively. The Eurogam detectors were positioned 205 mm from the target and the TESSA detectors were at a distance of 180 mm. Energy and efficiency calibrations were obtained with ^{133}Ba and ^{152}Eu radioactive sources placed at the JUROSPHERE target position. The total photopeak efficiency of the array was measured to be 1.5% at 1.3 MeV.

The recoiling fusion-evaporation residues entered the gas-filled recoil separator RITU [10], where they were separated from the beam and implanted into a 80 mm$\times$35 mm position-sensitive silicon strip detector at the separator's focal plane. The energy, position, and time of recoil implantations and the subsequently emitted α particles were recorded. γ rays detected at the target position in association with an evaporation residue being implanted into the silicon strip detector were also recorded. The position and time information recorded at the strip detector enabled α decays to be correlated with implanted recoils and thereby tag γ rays emitted by a specific nucleus.

In cases where two or more γ rays were detected simultaneously at the target position, their energies were also recorded. This allowed the evaporation residue transport efficiency of RITU to be determined for the strongest reaction channels from the proportion of their main γ-ray lines that also appeared in coincidence with a recoil ion in the silicon strip detector. In the case of ^{160}Hf, produced via the $4p$ evaporation channel, this was found to be $(21\pm1)\%$ at a beam energy of 291 MeV.

III. RESULTS

A. Nuclide ^{160}W

The energy spectrum of all γ rays observed in coincidence with a recoil ion at the focal plane of RITU is shown in Fig. 1(a). ^{160}W was produced with a cross section of $\sim$160 μb and is a known emitter of 5912 keV α particles, with a half-life of 91 ms and branching ratio of 87% [4]. The corresponding γ-ray energy spectrum obtained for those ions followed by a ^{160}W α decay within a maximum time interval of 455 ms at the same detector position is shown in Fig. 1(b). Although the peaks in this spectrum differ from those in Fig. 1(a), it is evident from the α-particle energy spectrum of Fig. 2 that the ^{160}W α line is not fully resolved from that of its daughter ^{156}Hf, which emits 5873 keV α particles with a half-life of 23 ms and branching ratio of 100% [4]. Furthermore, the relative intensity of the α-decay lines in Fig. 2 shows that ^{156}Hf is also produced directly via the $\alpha 2p2n$ evaporation channel. In order to eliminate the possibility that some of the tagged γ rays could be emitted by ^{156}Hf rather than ^{160}W, recoil-α-α correlations were performed, requiring that the ^{160}W α decays be followed by a position-correlated ^{156}Hf α decay within 65 ms. The resultant tagged γ-ray energy spectrum is shown in Fig. 1(c), in which the same γ-ray lines can be seen as in Fig. 1(b). Further corroboration of the assignment of these γ rays to ^{160}W comes from the observation of tungsten x rays in the tagged spectra and the absence of the γ rays previously assigned to ^{156}Hf [11].

In order to optimize statistics for the analysis of γ-γ coincidences, a γ-γ matrix was constructed for recoil-^{160}W α gated events having a γ-ray multiplicity $\geqslant 2$. The four strongest γ rays in Fig. 1(b) at 347 keV, 610 keV, 616 keV, and 655 keV are mutually coincident and are assumed to represent transitions between the lowest-lying states in ^{160}W. Figure 3(a) shows the summed energy spectrum of γ rays obtained by gating on each of these four transitions. Analysis of the coincidence relationships of these four γ rays reveals that they are in coincidence with all other transitions assigned to ^{160}W. Figure 3(b) shows the summed γ-ray energy spectrum obtained by gating on the mutually coincident 624 keV, 671 keV, and 696 keV transitions. Four additional weak γ-ray lines at energies of 460 keV, 544 keV, 573 keV, and 681 keV are evident in this spectrum. Gating on the mutually coincident 222 keV, 713 keV, and 718 keV transitions results in the γ-ray energy spectrum shown in Fig. 3(c), in which transitions at energies of 296 keV, 407 keV, 494 keV, and 853 keV can be identified, in addition to the four strongest ^{160}W γ rays. These γ-γ coincidence data indicate that

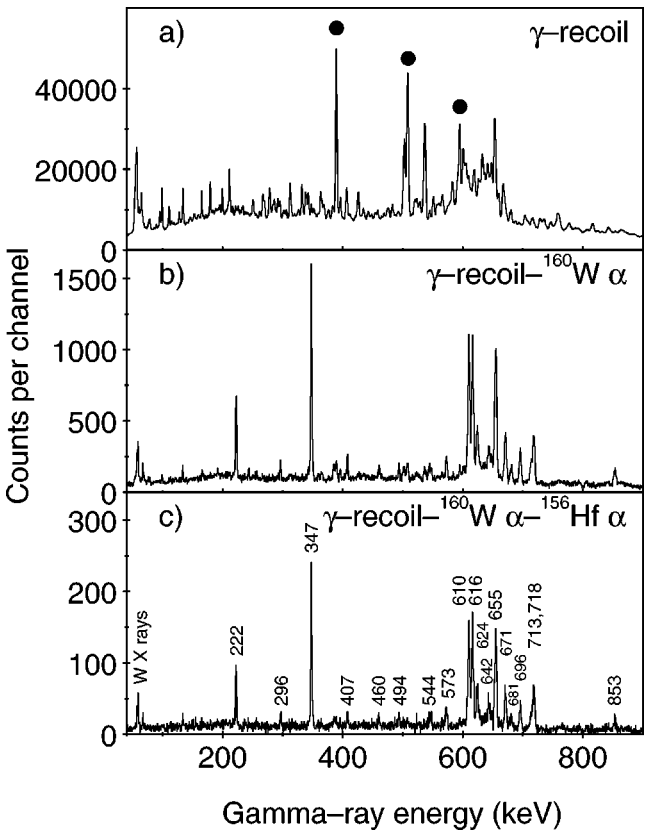

FIG. 1. Energy spectrum of (a) all γ rays associated with a recoil detected at the focal plane of RITU, (b) γ rays emitted by ions correlated with subsequent α decays in the ^{160}W peak, and (c) γ rays emitted by ions correlated with subsequent ^{160}W and ^{156}Hf α decays. These spectra represent the sum of data obtained at all three beam energies used in the present experiment. The known lowest transitions in ^{160}Hf [12], which was strongly produced via the $4p$ evaporation channel, are indicated by solid circles in (a), while γ rays assigned as transitions in ^{160}W are labeled with their energies in keV in (c). Only small vestiges of the ^{160}Hf γ rays can be discerned in (b) and (c), and arise from the low level of false correlations of α particles with unrelated ions.

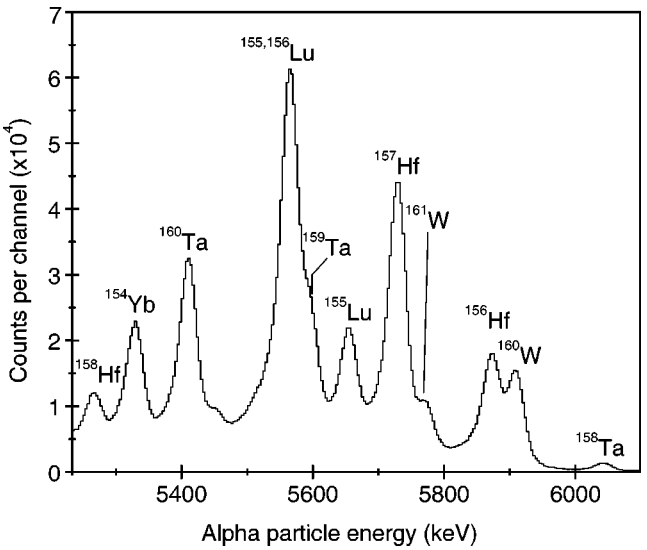

FIG. 2. A portion of the energy spectrum of α particles recorded at the beam energy of 291 MeV during beam-off periods in the position-sensitive silicon strip detector at the focal plane of RITU. The calibration was obtained using the energies of known α emitters produced in this reaction [4] and the strongest α-decay lines including those of interest in the present work are labeled.

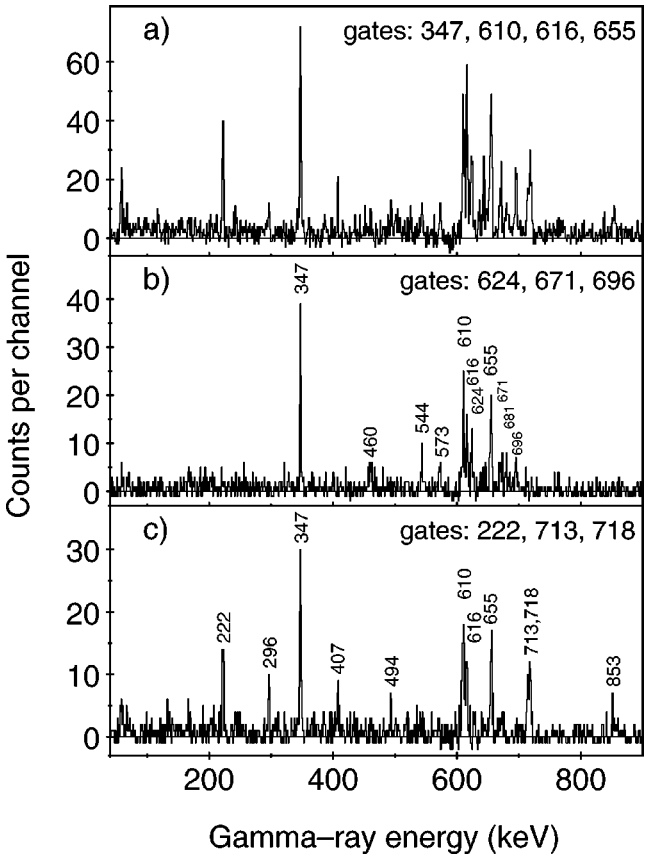

FIG. 3. Energy spectrum of ^{160}W γ rays observed in coincidence with (a) the 347 keV, 610 keV, 616 keV, and 655 keV transitions, (b) the 624 keV, 671 keV, and 696 keV transitions, and (c) the 222 keV, 713 keV, and 718 keV transitions.

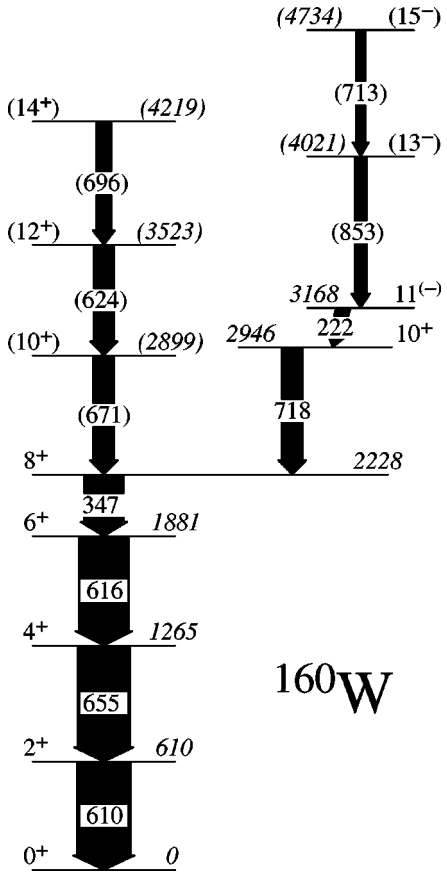

FIG. 4. The proposed partial level scheme for ^{160}W, deduced from the γ-γ coincidence relationships, angular distributions, and relative intensity measurements. The widths of the arrows are proportional to the transition intensity. Level energies are given in keV.

the level scheme of ^{160}W splits into two bands, as shown in Fig. 4.

Information on the multipolarity of the γ rays was deduced from a comparison of the ratio of peak intensities measured in the TESSA detectors at 79° and 101° to those measured in the Eurogam detectors at 157.6° (see Table I). The intensity ratios measured for the ^{160}W γ rays typically have values around 1.16, except for the 222 keV transition. However, the value for this transition of 0.88 ± 0.07 is consistent with that of 0.91 ± 0.05 measured for the 211.6 keV ^{160}Hf stretched dipole transition [12]. We therefore assign the 222 keV γ ray as a dipole, tentatively $E1$, transition and the remaining γ rays with measured intensity ratios as stretched $E2$ transitions. The choice of an $E1$ rather than an $M1$ transition for the 222 keV γ ray is in accordance with the energy level systematics of nuclei in the vicinity of ^{160}W, where the observed low-lying odd-spin bands are of negative parity.

The energies and relative intensities of γ rays attributed to ^{160}W are also presented in Table I. The transition intensities, after efficiency and internal conversion corrections, have been normalized to that of the 610 keV transition. To allow for the asymmetry of the JUROSPHERE array, the intensity of the 222 keV dipole transition has also been corrected by scaling according to the relative intensity measured for the

TABLE I. Transition energies, relative intensities corrected for internal conversion, intensity ratios, and spin assignments for γ rays attributed to ^{160}W.

Energy (keV)	Intensity [a]	R [b]	$J_i^\pi \rightarrow J_f^\pi$
222.1±0.2	25±3	0.88±0.07	$11^{(-)} \rightarrow 10^+$
295.9±0.2	6±2		
347.5±0.2	70±3	1.11±0.06	$8^+ \rightarrow 6^+$
407.4±0.2	10±2		
460.2±0.2	7±2		
493.6±0.2	8±2		
543.8±0.3	9±2		
572.6±0.2	12±2		
609.9±0.2	100±2	1.20±0.07[c]	$2^+ \rightarrow 0^+$
616.2±0.2	92±3	1.20±0.07[c]	$6^+ \rightarrow 4^+$
624.2±0.2	42±3[d]		$(12^+ \rightarrow 10^+)$
642.3±0.3	26±3[e]		$(16^+ \rightarrow 14^+)$
654.7±0.2	97±2	1.19±0.05	$4^+ \rightarrow 2^+$
670.7±0.2	39±3	1.03±0.09	$(10^+ \rightarrow 8^+)$
680.6±0.2	13±2		
695.6±0.2	28±3	1.23±0.12	$(14^+ \rightarrow 12^+)$
713.1±0.4	17±3	1.17±0.19	$(15^- \rightarrow 13^-)$
718.1±0.2	39±3	1.24±0.11	$10^+ \rightarrow 8^+$
853.5±0.3	22±2	1.04±0.13	$(13^- \rightarrow 11^-)$

[a]Normalized to the intensity of the 610 keV transition.
[b]Intensity ratio, $R = I_\gamma$ (157.6°) I_γ (79° and 101°).
[c]Average of both transitions.
[d]Unresolved doublet. Value given is the combined intensity of both transitions. The weaker component is estimated to represent ~10% of the combined intensity.
[e]Unresolved doublet. Value given is the combined intensity of both transitions.

211.6 keV ^{160}Hf dipole transition compared with the literature value [12]. The sequence of the transitions in the level scheme of Fig. 4 is tentative and follows the order of their relative intensities. The possible discrepancy in the intensity feeding into and out of the 8^+ level could be an indication that this level has a lifetime of the order of a few ns, perhaps arising as a consequence of a spin-flip transition to the 6^+ state and resulting in some γ rays being emitted after the nuclei have recoiled out of view of JUROSPHERE. The relative intensities of the 222 keV and 718 keV transitions indicates the existence of two closely spaced 10^+ levels, one of which is fed by the negative-parity states and the other by the positive-parity band.

B. Nuclide ^{159}Ta

One feature of tagging γ rays with the subsequent α decays of their associated recoil ions is that in some cases it is possible to select out specific configurations. An example of this is provided by ^{159}Ta produced via the $3p2n$ channel in the present work, for which two low-lying α-decaying levels are known: a low-spin level having an $s_{1/2}$ proton configuration and a high-spin $\pi h_{11/2}$ state [4]. The 544 ms half-life and 73% α-decay branching ratio of the $\pi h_{11/2}$ state [4] should make it a suitable candidate for the α-decay tagging technique. Proton- and α-decay measurements have determined that the $\pi s_{1/2}$ state represents the ground state of ^{159}Ta, with the $\pi h_{11/2}$ state lying at an excitation energy of 64±5 keV [13].

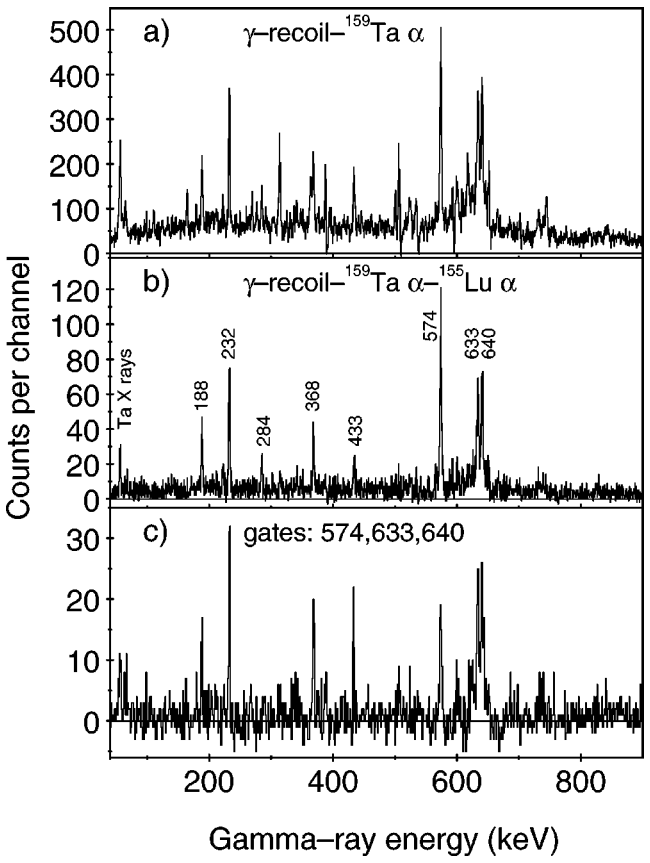

FIG. 5. Energy spectra of (a) γ rays emitted by ions correlated within 1.3 s with subsequent α decays in the ^{159}Ta peak, (b) γ rays emitted by ions that are in turn correlated within 200 ms with subsequent ^{155}Lu α decays, and (c) γ rays observed in coincidence with the 574 keV, 633 keV, and 640 keV transitions in the recoil-α gated γ-γ matrix for ^{159}Ta. Since the $\pi h_{11/2}$ level in ^{159}Ta has a half-life of ~500 ms, it was also necessary to subtract a fraction of the total recoil–γ-ray spectrum from both (a) and (b) in order to eliminate contributions from random correlations. Peaks assigned to ^{159}Ta are labeled in (b) with their energy in keV. These spectra represent the sum of data obtained at all three-beam energies used in the present experiment.

In the present data, the 5.6 MeV α decays of the $\pi h_{11/2}$ state were produced strongly, but could not be resolved from other α lines of similar energy (see Fig. 2). However, this α decay populates the low-lying $\pi h_{11/2}$ state in ^{155}Lu, which in turn decays by emitting 5655 keV α particles and has a half-life of 70 ms and branching ratio of 80% [4]. This correlation is sufficient to select out cleanly the ^{159}Ta α decays of interest and the corresponding γ-ray energy spectrum is shown in Fig. 5(b). It is evident that some of the γ rays present in the recoil-α tagged spectrum of Fig. 5(a) are removed by correlation with the second α decay and the appearance of tantalum x rays in Fig. 5(b) corroborates the assignment of γ rays to ^{159}Ta. Analysis of the recoil-α gated γ-γ coincidences confirms that the 574 keV, 633 keV, and

TABLE II. Transition energies, relative intensities corrected for internal conversion, and tentative spin assignments for γ rays assigned to ^{159}Ta.

Energy (keV)	Intensity [a]	$J_i^\pi \rightarrow J_f^\pi$
188.3±0.1	12±2	
232.4±0.1	40±4	
284.2±0.1	7±2	
368.3±0.1	24±3	
433.5±0.2	15±3	
573.7±0.1	100±2	$(15/2^- \rightarrow 11/2^-)$
633.4±0.1	72±6	$(23/2^- \rightarrow 19/2^-)$
640.5±0.1	86±5	$(19/2^- \rightarrow 15/2^-)$

[a]Normalized to the intensity of the 574 keV transition.

640 keV transitions are mutually coincident. Figure 5(c) shows the summed energy spectrum of γ rays obtained by gating on each of these three transitions. This demonstrates that they are in coincidence with all other transitions assigned to ^{159}Ta. The statistics were not sufficient to allow placement of the ^{159}Ta γ-ray transitions at 188 keV, 232 keV, 284 keV, 368 keV, and 433 keV in the level scheme.

The angular distributions of the γ rays suggests that the 232 keV γ ray is a dipole transition and all other peaks are consistent with stretched quadrupole transitions. The energies and efficiency-corrected intensities of the γ rays in the spectrum of Fig. 5(b) are listed in Table II. The three most intense transitions at 574 keV, 633 keV, and 640 keV are assumed to represent transitions between the lowest-lying states built on the $\pi h_{11/2}$ level in ^{159}Ta, as illustrated in the tentative partial level scheme shown in Fig. 6.

IV. DISCUSSION

The angular momentum of low-lying excited states in even-even nuclei close to the $N=82$ shell closure is generated by spin alignments of individual valence nucleons. In $N=82$ nuclei, the yrast states are formed by $\pi(h_{11/2})^n$ configurations, with two proton excitations being mainly responsible for levels up to the maximally aligned 10^+ state [14], while in $N=84$ isotones these configurations are coupled

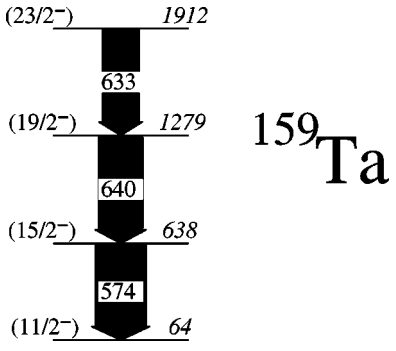

FIG. 6. The tentative partial level scheme for ^{159}Ta, deduced from the relative intensity measurements and coincidence relationships. The excitation energy of the $\pi h_{11/2}$ bandhead is 64 ±5 keV [13].

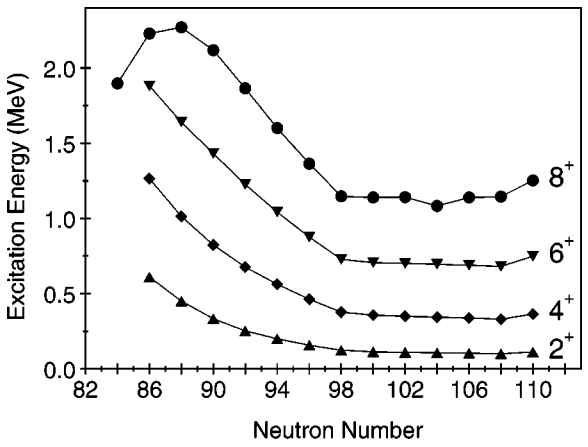

FIG. 7. Excitation energies of low-lying positive-parity levels in even-even tungsten isotopes as a function of neutron number. Data are taken from Refs. [4–6,18] and the present work.

with $\nu(f_{7/2}^2)$ and $\nu(f_{7/2}h_{9/2})$ excitations to form the lowest-lying positive-parity states [15]. Negative-parity states can be generated by $\nu(i_{13/2}h_{9/2})$, $\pi(h_{11/2}d_{5/2})$, and $\pi(h_{11/2}s_{1/2})$ excitations. In $N=86$ isotones, these basic excitation patterns can still be discerned [16,17], but for still higher neutron numbers, nuclei become increasingly collective.

This emergence of the importance of individual nucleon excitations is evident in the excitation energy systematics of low-lying positive-parity states in even-mass tungsten isotopes, shown in Fig. 7. The energies of the 2^+, 4^+, and 6^+ levels determined in the present work for ^{160}W represent a smooth continuation of the trend of increasing excitation energy and hence decreasing deformation with decreasing neutron number. This contrasts with the 8^+ levels, which fall below the extrapolated trend for $N<90$. This behavior can be attributed to a maximally aligned $\nu(f_{7/2}h_{9/2})_8^{max}$ or $\nu(h_{9/2}^2)_8^{max}$ excitation, which becomes increasingly favored energetically as the $N=82$ shell closure is approached [19]. The energy of the 8^+ level measured for ^{160}W provides a gradual evolution to that in ^{158}W, where it falls below the 6^+ level and becomes isomeric, decaying by α-particle emission [4,19].

The corresponding energy level systematics for even-mass $N=86$ nuclei shown in Fig. 8 reveal a fairly regular spacing of the 2^+, 4^+, and 6^+ levels in these isotones, with transition energies of $\sim$600 keV. The energy of the 8^+ level decreases slightly with increasing atomic number, reflecting an increasing energy gain by the interaction of $h_{9/2}$ neutrons with $h_{11/2}$ protons as the $\pi h_{11/2}$ subshell is filled [19]. The 10^+ levels also show a smooth decrease with increasing Z, reflecting the trend identified for the $\pi(h_{11/2}^2)_{10}^{max}$ 10^+ isomers in $N=82$ isotones [14]. The low-lying positive-parity states deduced in the present work for ^{160}W fit in well with these systematics.

Negative-parity 11^- states have been observed in $N=86$ isotones at a comparable energy to that identified in ^{160}W. A g-factor measurement for the 3025 keV level in ^{154}Er indicated that the main configuration of this 11^- state is a $\nu(i_{13/2}h_{9/2})$ excitation [20] and it seems reasonable to attribute the states seen in other isotones to this excitation [16].

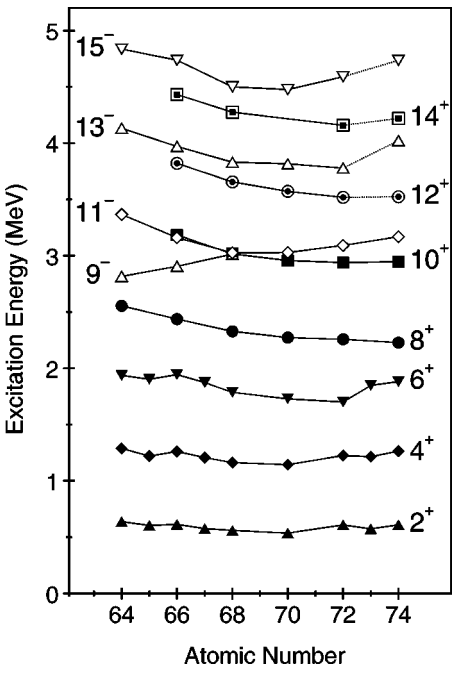

FIG. 8. Excitation energies of low-lying levels in even-mass $N=86$ isotones as a function of atomic number. For the odd-Z elements, the energy levels shown represent the lowest levels built upon $\pi h_{11/2}$ configurations. Data are taken from Refs. [5,18] and the present work. The lines are drawn to guide the eye, with the dotted lines connecting the levels tentatively proposed in the present work.

In ^{154}Er, ^{156}Yb, and ^{158}Hf, the 11^- states are observed to decay strongly to 10^+ levels by $E1$ transitions [5,16,17], a pattern which appears to be followed in ^{160}W. In ^{154}Er and the lighter isotones, there is a decay from the 11^- state to a 9^- level, which then feeds lower-spin negative-parity states. These states are thought to be built mainly upon a $\pi(h_{11/2}d_{5/2}^{-1})$ excitation, which becomes progressively blocked as the $\pi h_{11/2}$ subshell is filled and the excitation energies consequently increase (see Fig. 8). In ^{156}Yb, the nonobservation of lower-spin negative-parity states is presumed to be a result of the 9^- state lying above the 11^- and not being strongly populated [16]. This explanation would naturally account for the similar pattern observed for ^{160}W in the present work.

In the odd-mass $N=86$ isotones studied to date, the odd $\pi h_{11/2}$ proton is coupled to the low-lying excitations seen in neighboring isotones [21,22]. The excitation energies of the states identified in ^{159}Ta in the present work also fit into this pattern, being comparable with the corresponding levels in ^{158}Hf and ^{160}W (see Fig. 8). It would certainly be of interest to extend the level scheme of ^{159}Ta in order to pursue this comparison to higher spins.

V. CONCLUSION

The γ rays emitted from excited states in the neutron deficient nuclei ^{159}Ta and ^{160}W have been identified for the first time by tagging the recoil ions emitting the γ rays with both parent and daughter α decays. A level scheme has been deduced for ^{160}W and interpreted in terms of the neutron excitations outside the $N=82$ core seen in its $N=86$ isotones and the $\pi h_{11/2}$ proton excitations observed in neighboring nuclei. The lowest transitions based on the $\pi h_{11/2}$ configuration in ^{159}Ta are found to follow closely the excitation energies of the corresponding transitions in the neighboring isotones.

ACKNOWLEDGMENTS

Support for this work was provided by the U.K. Engineering and Physical Sciences Research Council and the Academy of Finland. P.T.G., A.K., S.L.K., R.D.P., and M.J.T. acknowledge financial support from EPSRC. We would like to thank the staff at JYFL for providing the beam and their excellent technical support. We also thank the French/U.K. (IN2P3/EPSRC) Loan Pool for the Eurogam detectors of JUROSPHERE.

[1] S.L. King *et al.*, Phys. Lett. B **443**, 82 (1998).
[2] M. Muikku *et al.*, Phys. Rev. C **58**, R3033 (1998).
[3] J.F.C. Cocks *et al.*, Eur. Phys. J. A **3**, 17 (1998).
[4] R.D. Page *et al.*, Phys. Rev. C **53**, 660 (1996).
[5] G.D. Dracoulis *et al.*, in Proceedings of the International Conference of Nuclear Structure at High Angular Momentum, Ottawa, 1992, AECL Report No. 10613 (unpublished), Vol. 2, p. 94.
[6] J. Simpson *et al.*, J. Phys. G **17**, 511 (1991).
[7] D.G. Roux *et al.*, Phys. Rev. C **63**, 024303 (2001).
[8] C.W. Beausang *et al.*, Nucl. Instrum. Methods Phys. Res. A **313**, 37 (1992).
[9] P.J. Nolan, D.W. Gifford, and P.J. Twin, Nucl. Instrum. Methods Phys. Res. A **236**, 95 (1985).
[10] M. Leino *et al.*, Nucl. Instrum. Methods Phys. Res. B **99**, 653 (1995).
[11] M.P. Carpenter *et al.*, Z. Phys. A **358**, 261 (1997).
[12] M. Murzel *et al.*, Nucl. Phys. **A516**, 189 (1990).
[13] C.N. Davids *et al.*, Phys. Rev. C **55**, 2255 (1997).
[14] J.H. McNeill *et al.*, Phys. Rev. Lett. **63**, 860 (1989).
[15] C.T. Zhang *et al.*, Phys. Rev. C **54**, R1 (1996).
[16] C.J. Lister *et al.*, Phys. Rev. C **23**, 2078 (1981).
[17] C. Schück *et al.*, Nucl. Phys. **A496**, 385 (1989).
[18] *Table of Isotopes*, 8th ed., edited by R.B. Firestone, V.S. Shirley, C.M. Baglin, S.Y.F. Chu, and J. Zipkin (Wiley, New York, 1996), Vol. 2.
[19] S. Hofmann *et al.*, Z. Phys. A **333**, 107 (1989).
[20] L. Nguyen *et al.*, Z. Phys. A **309**, 207 (1983).
[21] P. Kemnitz *et al.*, Nucl. Phys. **A311**, 11 (1978).
[22] D.C. Radford *et al.*, Phys. Lett. **126B**, 24 (1983).